

1 **Climate Change and Downstream Water Quality in Agricultural Production:**  
2 **The Case of Nutrient Runoff to the Gulf of Mexico**

3  
4 Levan Elbakidze<sup>a,b\*</sup>  
5 Associate Professor  
6 [levan.elbakidze@mail.wvu.edu](mailto:levan.elbakidze@mail.wvu.edu)

7  
8 Yuelu Xu<sup>a</sup>  
9 Post-Doctoral Fellow  
10 [yuelu.xu@mail.wvu.edu](mailto:yuelu.xu@mail.wvu.edu)

11  
12 Philip W. Gassman<sup>c</sup>  
13 Associate Scientist  
14 [pwgassma@iastate.edu](mailto:pwgassma@iastate.edu)

15  
16 Jeffrey G. Arnold<sup>d</sup>  
17 Agricultural Engineer  
18 [jeff.arnold@usda.gov](mailto:jeff.arnold@usda.gov)

19  
20 Haw Yen<sup>e,f</sup>  
21 Senior Scientist  
22 [haw.yen@gmail.com](mailto:haw.yen@gmail.com)

23  
24 <sup>a</sup> Division of Resource Economics and Management, Davis College of Agriculture,  
25 Natural Resources and Design, West Virginia University, Agricultural Sciences  
26 Building, Morgantown, West Virginia 26506, USA.

27 <sup>b</sup> Center for Innovation in Gas Research and Utilization, West Virginia University,  
28 Morgantown, West Virginia 26506, USA.

29 <sup>c</sup> Center for Agricultural and Rural Development, Iowa State University, Ames, Iowa  
30 50011, USA.

31 <sup>d</sup> Grassland Soil and Water Research Laboratory, USDA-ARS, Temple, Texas 76502,  
32 USA.

33 <sup>e</sup> Crop Science, Bayer U.S., 700 W Chesterfield Pkwy W, Chesterfield, Missouri  
34 63017, USA.

35 <sup>f</sup> School of Forestry & Wildlife Science, Auburn University, Auburn, Alabama 36849,  
36 USA.

37 \*Corresponding author

38  
39  
40  
41  
42  
43

44

45 **Abstract**

46 Nitrogen (N) fertilizer use in agricultural production is a significant determinant  
47 of surface water quality. As climate changes, agricultural producers are likely to adapt  
48 at extensive and intensive margins in terms of planted acreage and per ha input use,  
49 including fertilizers. These changes can affect downstream water quality. We  
50 investigate the effect of climate-driven land productivity changes on water quality in  
51 the Gulf of Mexico using an integrated hydro-economic agricultural land use (IHEAL)  
52 model. Our results indicate that land and N use adaptation in agricultural production  
53 to climate change increases N delivery to the Gulf of Mexico by 0.5%-1.6% (1,690  
54 -5,980 metric tons) relative to the baseline scenario with no climate change.

55

56 **1. Introduction**

57 Mississippi River Basin (MRB) spans more than 3.2 million square kilometers, is  
58 dominated by agricultural land use, and is the largest drainage basin in the U.S.  
59 Approximately 70% of U.S. cropland is in the MRB (Kumar and Merwade, 2011;  
60 Marshall et al., 2018). Agricultural production in the MRB relies on intensive nitrogen  
61 (N) fertilizer use with a well-documented negative externality in the form of Hypoxia  
62 in the Gulf of Mexico.

63 Hypoxia in the Gulf has been a public concern for decades due to the detrimental  
64 consequences for the aquatic ecosystems (US EPA, 2019). N runoff to the Gulf and  
65 the consequent eutrophication of coastal waters promotes algal bloom. Decomposing  
66 algae depletes the marine ecosystem of dissolved oxygen, which is critical for  
67 sustaining aquatic ecosystems. Oxygen depletion results in hypoxic or “dead” zones  
68 as marine life either dies or migrates to other areas. In 2001, the EPA established the  
69 Gulf of Mexico Hypoxia Task Force to reduce the size of the Hypoxic zone to 5,000  
70 km<sup>2</sup> by 2035 (US EPA, 2014). In 2021, the hypoxic zone in the Gulf still reached  
71 16,405 km<sup>2</sup>, significantly exceeding the EPA goal (US EPA, 2021a).

72 Climate change, with higher temperatures, more variable rainfall, and elevated

73 CO<sub>2</sub> concentrations, can substantially affect crop yields and agricultural production.  
74 Previous literature documents mixed expected impacts of climate change on crop  
75 yields in the MRB. Panagopoulos et al. (2014) simulated corn and soybean yields in  
76 the Upper Mississippi River Basin (UMRB, a subbasin of the MRB) using the Soil  
77 and Water Assessment Tool (SWAT) for the baseline climate (1981-2000) and seven  
78 future (2046-2065) GCM climate projections under four agricultural management  
79 scenarios. Predicted corn and soybean yields modestly decline relative to the baseline  
80 climate conditions under all future climates and agricultural management scenarios.  
81 Panagopoulos et al. (2015) reported similar results for the Ohio-Tennessee River  
82 Basin (OTRB, a subbasin of the MRB), with predicted corn and soybean yields in all  
83 examined future climates and agricultural management practices declining relative to  
84 the corresponding baseline scenarios. Chen et al. (2019) modeled the effects of  
85 climate change on crop yields in the Northern High Plains of Texas (partially located  
86 within the MRB) using the SWAT. They found that the median irrigated corn and  
87 sorghum yields would decrease by 3%-22% and 6%-42%, respectively, relative to the  
88 historical values. Median non-irrigated sorghum yield would decrease by up to 10%.

89       The changes in crop yields in the MRB may influence agricultural input and land  
90 use with associated implications for environmental outcomes in the Gulf of Mexico.  
91 On the one hand, the use of N fertilizer may intensify to compensate for losses in crop  
92 yields. This may increase N runoff from the MRB and exacerbate Hypoxia in the Gulf  
93 of Mexico. On the other hand, lower yields may reduce profitability of crop  
94 production and may result in decreased crop acreage, which could decrease N runoff  
95 to the Gulf of Mexico. The net effect of climate change-driven changes in crop yields  
96 on N runoff to the Gulf of Mexico is thus unclear and should be examined  
97 empirically.

98       The MRB is the largest basin in the U.S. and includes several large sub-basins  
99 with different agricultural practices and contributions to the Gulf N runoff. For  
100 example, UMRB and OTRB are major N contributors to the Gulf (Kling et al., 2014;

101 White et al., 2014). In the Corn Belt, highly fertile soils, relatively level land, hot days  
102 and nights, and well-distributed precipitation during the growing season provide ideal  
103 conditions for crop production (Wu et al., 2015). These factors have led to prevalent  
104 corn-soybean rotation with high fertilizer use and tile drainage systems. The Missouri  
105 and Arkansas-Red-White River Basin includes both rainfed and irrigated crop  
106 production. In Nebraska, western Kansas, Oklahoma and north Texas, groundwater  
107 from Ogallala aquifer is a major source of irrigation for agricultural production (Xu et  
108 al. 2022). Some of the climate projection scenarios suggest that regions with rainfed  
109 agriculture will be wetter and regions relying on irrigation will be drier (NCAR,  
110 2022a). These spatially heterogeneous changes, and the corresponding adaptations,  
111 are important to examine in terms of implications for environmental outcomes.

112 The MRB contains 962,342 square kilometers of cropland. Corn, soybean, and  
113 wheat are dominant crops, which account for 34.6%, 23.1%, and 18.0% of cropland,  
114 respectively (Marshall et al., 2018). Figure 1 presents the harvested acreages of major  
115 crops planted in the MRB from 1997 to 2017 (USDA NASS, 2019). Corn and  
116 soybean acreages increased substantially over time mainly due to the increasing  
117 demand for feedstock sources in bioenergy production and feed for both domestic and  
118 overseas livestock operations (USDA ERS, 2022). Meanwhile, wheat and sorghum  
119 acreages have decreased. Correspondingly, irrigated corn and soybean acreages grew  
120 significantly from 1997 to 2017, while irrigated wheat and sorghum acreages declined  
121 (Figure 2).

122 There are several farmer adaptation options to climate-driven changes in crop  
123 yields. For example, technological developments, government and insurance  
124 programs, alternative farm production practices like new irrigation systems, and more  
125 drought tolerant crops can mitigate some of the climate impacts on agriculture (Smit  
126 and Skinner, 2002). While these options are important for a comprehensive  
127 examination, in this study, we offer a partial analysis of farmers' response to climate  
128 driven changes in crop yields. We examine adaptation at the extensive (planting

129 decisions for existing crops) and intensive (per ha nitrogen use and irrigation) margins,  
130 *ceteris paribus*. This analysis offers an initial assessment of the relationship between  
131 N runoff and adaptation in agricultural production to climate change. Future studies  
132 should consider a wider set of adaptation alternatives including new crop varieties and  
133 production technologies.

134 While there is extensive literature on the impacts of agricultural production on N  
135 loading in surface water, few studies have evaluated this problem in the context of  
136 climate change. Bosch et al. (2018) and Xu et al. (2019) evaluated the effects of  
137 climate change on the costs of achieving water quality goals in an experimental  
138 watershed in Pennsylvania using an economic model and the SWAT-Variable Source  
139 Area model with climate predictions. Both studies showed that estimated costs of  
140 meeting water quality goals increase in future climates relative to the historical  
141 baseline. However, N fertilizer use in these studies is exogenously determined, which  
142 limits N use flexibility in response to variations in crop yields in future climate  
143 scenarios.

144 We contribute to previous literature by examining the effects of climate change  
145 on N runoff to the Gulf of Mexico with endogenous land and N use decisions. Our  
146 approach includes a behavioral crop production response to changes in productivity  
147 and evaluates N runoff accordingly. Our focus is on N and land use with associated  
148 impacts on N runoff to the Gulf, as a response to crop yield changes in future climate  
149 scenarios. Our primary purpose is to draw attention to the implications of adaptation  
150 to climate change in agricultural production for N use and downstream water quality.  
151 This aspect of climate change and associated adaptation has not received much  
152 attention in scientific literature. It is important to note that the objective of this study  
153 is not to predict the changes in N runoff to the Gulf under a changing climate, as the  
154 modeling exercise is based on several important assumptions and limitations that we  
155 discuss in the conclusions section. Instead, our goal is to provide a first, partial  
156 assessment of the sensitivity of Gulf N runoff to the changes in crop yields and

157 corresponding adaptation in crop production for some mid-century (2050-2068)  
158 climate change scenarios. The results of this study should encourage additional  
159 analysis of changes in N runoff as an externality from agricultural production  
160 adaptation to climate change.

161

## 162 **2. Theoretical Framework**

163 This section presents a theoretical economic framework and simplified analytical  
164 results illustrating the impact of climate driven changes in crop yields on fertilizer use.  
165 A parsimonious welfare maximization model with a representative commodity market  
166 is considered as:

167

$$\max_{x, n_1, n_2, w_1} \pi = \int_0^x p(t) dt - C_n * (n_1 + n_2) - C_w * w_1 \quad (1)$$

168

subject to

$$\alpha_1 * f(n_1, w_1) + \alpha_2 * g(n_2) \geq x \quad (2)$$

169 where  $x$  is crop consumption  $p(t)$  is the inverse commodity demand function.  $C_n$   
170 and  $C_w$  are unit costs for fertilizer and water, respectively. Crop production takes  
171 place in irrigated region 1 and rainfed region 2.  $f(n_1, w_1)$  is production function in  
172 region 1 requiring nitrogen ( $n_1$ ) and water ( $w_1$ ) as input factors, with  $f' > 0$ , and  
173  $f'' < 0$ .  $g(n_2)$  is production function in region 2 only requiring only nitrogen ( $n_2$ ),  
174 with  $g' > 0$ , and  $g'' < 0$ . For example, corn production in Illinois is mostly rainfed,  
175 while irrigated corn is prevalent in Kansas and Nebraska.  $\alpha_1$  and  $\alpha_2$  is the yield  
176 multiplier in future climates, with  $\alpha > 1$  indicating an increase in crop yield and  
177  $0 < \alpha < 1$  indicating a reduction in crop yield. Equations (2) limits crop  
178 consumption to not exceed production.

179 The appendix provides the Lagrangian and the first-order conditions, which are  
180 used to form the Hessian matrix. The determinant of the Hessian matrix is:

$$|H| = \alpha_1^2 \alpha_2 \lambda^2 \left[ 2\alpha_1 f_{n_1} f_{n_1 w_1} f_{w_1} g_{n_2 n_2} p_x - \alpha_1 f_{n_1}^2 f_{w_1 w_1} g_{n_2 n_2} p_x \right. \\ \left. + f_{n_1 w_1}^2 (\lambda g_{n_2 n_2} + \alpha_2 p_x g_{n_2}^2) \right. \\ \left. - f_{n_1 n_1} (\lambda f_{w_1 w_1} g_{n_2 n_2} + \alpha_2 f_{w_1 w_1} p_x g_{n_2}^2 + \alpha_1 f_{w_1}^2 g_{n_2 n_2} p_x) \right]$$

181 Comparative statics for changes in variables of interest with respect to the change in  
182  $\alpha_1$  are obtained using Cramer's rule:

183

$$\frac{\partial n_1}{\partial \alpha_1} = \frac{-\alpha_1 \alpha_2 \lambda^2 (f_{n_1 w_1} f_{w_1} - f_{n_1} f_{w_1 w_1}) (\alpha_2 p_x g_{n_2}^2 + g_{n_2 n_2} (\lambda + \alpha_1 p_x f(n_1, w_1)))}{|H|} \quad (3)$$

184

$$\frac{\partial n_2}{\partial \alpha_1} = \frac{-\alpha_1^2 \alpha_2 \lambda^2 g_{n_2} p_x [-2f_{n_1} f_{n_1 w_1} f_{w_1} + f_{n_1 n_1} f_{w_1}^2 + f(n_1, w_1) (f_{n_1 w_1}^2 - f_{n_1 n_1} f_{w_1 w_1})]}{|H|} \quad (4)$$

185

$$\frac{\partial w_1}{\partial \alpha_1} = \frac{-\lambda^2 \alpha_1 \alpha_2 (f_{n_1 w_1} f_{n_1} - f_{w_1} f_{n_1 n_1}) (\alpha_2 p_x g_{n_2}^2 + g_{n_2 n_2} (\lambda + \alpha_1 p_x f(n_1, w_1)))}{|H|} \quad (5)$$

186

187 The denominator  $|H|$  in equations (3), (4) and (5) is positive according to the  
188 maximization requirements. Therefore, the sign of equation (3), which shows the  
189 effects of changes in crop yields in region 1 on the N use in region 1, depends on the  
190 signs of the numerator. The direction of the derivative is indeterminate and depends  
191 on the slope of the demand curve, production function, change in yield, and price of  
192 the commodity. The sign of equation (4), indicating the effects of changes in crop  
193 yields in region 1 on N use in region 2, is also ambiguous and depends on the relative  
194 magnitudes of commodity price, yield and yield changes with respect to irrigation and  
195 fertilizer, and slope of the demand curve. Similar results can be observed for  
196 productivity changes in region 2 ( $\alpha_2$ ) and are provided in the appendix. Since nutrient  
197 runoff to the Gulf depends on per ha use of N and on acreage decisions, the combined  
198 effect of changes in productivity ( $\alpha$ ) on N runoff is ambiguous.

199 The sign of equation (5), which shows the effects of changes in crop yields in  
200 region 1 on water use in region 1, is also ambiguous. The direction of the change in

201 water use in region 1 under climate change depends on the production function, the  
202 price of the commodity, and magnitudes of changes in both crop yields. Similar  
203 results hold for the effect of region to yield changes ( $\alpha_2$ ) on water use in region 1  
204 (see appendix).

205 The simplified analytical model provides a theoretical insight for the effect of  
206 altered crop yields on input use as a form of adaptation to climate change. The result  
207 shows theoretical foundations for the need to consider the behavioral response to  
208 climate change alongside biophysical parameters in assessing the impacts of changes  
209 in production environment on production decisions that generate externalities for  
210 downstream water quality. Economic factors including prices and demand, and  
211 biophysical production parameters determine the first order conditions. Therefore,  
212 rigorous assessments of changes in N runoff from agricultural production in response  
213 to climate change should combine biophysical and economic modeling systems that  
214 account for adaptation in production activities. For the sake of parsimony, the  
215 theoretical analysis only considers two regions and a representative commodity rather  
216 than a set of crops, which is important to consider empirically as relocation of crop  
217 production will alter spatial N use distribution and runoff to the Gulf. In the empirical  
218 analysis, we use a spatially explicit model with four N intensive crops that combines  
219 biophysical and economic components to examine changes in N runoff.

220

### 221 **3. Methods and data**

222 We use the IHEAL model (Xu et al., 2022) to empirically assess the effects of  
223 climate change-driven crop yield variation on N runoff to the Gulf of Mexico. IHEAL  
224 is an integrated hydro-economic agricultural land use model, which combines a  
225 national price endogenous partial equilibrium commodity market formulation for  
226 select crops and a process-based SWAT. Corn, soybean, wheat and sorghum are  
227 included in the model as individual commodities because these crops are the most  
228 fertilizer-intensive crops planted in the U.S. (USDA NASS, 2020; Marshall et al.,  
229 2015; Steiner et al., 2021). Production of all other commodities is combined to



230 account for county-scale agricultural land use. The model includes county-scale crop  
231 planting, fertilizer use, and irrigation decisions. Production activities generate national  
232 commodity supply estimates that are combined with corresponding national  
233 commodity demand functions to produce equilibrium prices, quantities, and producer  
234 and consumer surplus estimates. The model endogenously determines annual county  
235 crop planting acreage, N use, and irrigation based on constrained consumer and  
236 producer welfare maximization in the select crop markets.

237 The IHEAL model maximizes consumer and producer welfare in the U.S. subject  
238 to commodity specific supply-demand balance, including exports and imports,  
239 production technology constraints, irrigated acreage constraints, and land allocation  
240 constraints that represent a convex combination of historically observed and synthetic  
241 county crop acreages. Historical and synthetic crop acreage proportions at the county  
242 scale are used to constrain planting decisions, so that model solutions reflect  
243 agronomic, managerial and technologic requirements for crop rotation. Synthetic  
244 acreages are obtained using own and cross-price elasticities and own and cross  
245 acreage price elasticities following Chen and Onal (2012). Elasticity estimates are  
246 obtained using fixed effect Arellano-Bond estimator and county production and price  
247 data from 2005 to 2019.

248 HAWQS platform is used to obtain SWAT long-run crop yields and N runoff to  
249 the Gulf for the baseline time period (2000-2018) (HAWQS, 2020). HAWQS platform  
250 also provides future (2050-2068) crop yields for five different Coupled Model  
251 Intercomparison Project Phase 5 (CMIP5) climate models, including ACCESS1.3,  
252 MIROC5, IPSL-CM5A-LR, MIROC-ESM-CHEM and CCSM4<sup>1</sup>. Table 1 presents the  
253 list of climate models used in this study. The performance of the selected climate  
254 models is discussed in Harding et al. (2013). Figure 3 presents average crop yields  
255 across all counties within the MRB under baseline (historical) and future climate  
256 scenarios. The “Ensemble” scenario is the mean across all climate change models.

---

<sup>1</sup> The climate models in our study were selected based on the availability in HAWQS, and inclusion in Harding et al. (2013) assessment.

257 The impacts of climate change on corn yields are negative in all climate scenarios  
258 relative to the baseline, which is consistent with previous literature (Panagopoulos et  
259 al., 2014, 2015; Chen et al., 2019). The impacts on soybean, wheat and sorghum  
260 yields are mixed across climate models.

261 The IHEAL model includes crop production activities in 2,788 counties in the  
262 contiguous U.S. where at least one of the crops included in this model was planted in  
263 at least one year from 2005 to 2019. These counties include 1,620 that are located  
264 within MRB and 1,168 outside. Per ha crop yields in the counties located within MRB  
265 are expressed as functions of N use and irrigation using SWAT parameters. Per ha  
266 crop yields in counties outside of MRB are fixed based on the USDA data and do not  
267 vary with irrigation and N use. Instead, to account for the aggregate impact of climate  
268 change on yields outside the MRB, we discount corn, soybean, and sorghum yields by  
269 1.6%, 2.7%, and 6%, respectively, and increase wheat yields by 7% relative to their  
270 corresponding baseline values (Basche et al., 2016; Karimi et al., 2017; Chen et al.,  
271 2019). County planted acreages within and outside of MRB are endogenously  
272 estimated.

273 The parametric model data include crop demand elasticities, market prices,  
274 county-specific historical crop acreage, historical county maximum irrigated acreage,  
275 and input costs, including energy, fertilizer, water and other production costs. The  
276 crop demand elasticities are obtained from previous literature (Westcott and Hoffman,  
277 1999; Piggott and Wohlgenant, 2002; Ishida and Jaime, 2015). The crop market prices  
278 and historical crop acreage are collected from USDA NASS (USDA NASS, 2020).  
279 The county maximum observed irrigated acreages are obtained from U.S. Geological  
280 Survey data (Dieter et al., 2018; USGS, 2018). The upper bounds on county scale  
281 irrigated acreage restrict model solutions from irrigating lands that have never been  
282 irrigated due to water, water right, and/or capital limitations. Energy input, fertilizer,  
283 water and other production costs are obtained from USDA ERS (USDA ERS, 2019).  
284 IHEAL combines county production activities, including crop planting acreage,  
285 irrigation, fertilizer use and leaching with the watershed SWAT delivery ratios to

286 estimate annual N runoff from crop production to the Gulf of Mexico (White et al.,  
287 2014).

288

#### 289 **4. Results and discussion**

290 Section 4 is organized as follows. We first present the validation and baseline  
291 results. Next, we discuss aggregate MRB results for crop production and N runoff  
292 with adjusted crop yields within the MRB under future climate scenarios. Then, we  
293 evaluate crop production and N runoff to the MRB under altered precipitation within  
294 the MRB and crop yields outside the MRB in future climates. Finally, we present the  
295 corresponding spatial results for the changes in N use and delivery to the Gulf of  
296 Mexico relative to the baseline values.

297

##### 298 **4.1 Validation and baseline results**

299 The purpose of this section is twofold. One is to validate the model solutions in  
300 terms of replicating observed market data. The other is to obtain baseline estimates of  
301 N runoff to the Gulf, to be used as benchmarks for subsequent climate scenario  
302 analyses.

303 For model validation purposes, the model is solved using observed county  
304 historical crop mix data. We present the 2018 observed values and the corresponding  
305 key baseline model solutions, including crop production, crop prices, the amount of N  
306 delivered to the Gulf of Mexico, irrigated crop acreage, and the irrigation water used  
307 for corn, soybean, sorghum, and wheat within the MRB as part of model validation  
308 (Table 2). The model overestimates cumulative crop acreage for corn, soybean, wheat  
309 and sorghum by 10.0%, 8.3%, 9.9% and 4.4%, respectively, relative to the acreages  
310 observed in 2018. All estimated crop prices are close to the observed values in 2018,  
311 with all deviations less than 3%.

312 Baseline water use, N use and N delivery to the Gulf of Mexico are also  
313 presented in Table 2. The estimated irrigated acreage of corn, soybean, wheat and  
314 sorghum within the MRB is 3.92 million ha, representing 65.93% of irrigated acreage

315 for these crops in the U.S. in 2018. The annual water use within the MRB is 4.52  
316 million acre-feet, which accounts for 5.42%<sup>2</sup> of the total observed irrigation water  
317 use in the U.S. Annual N use within the MRB for corn, soybean, wheat and sorghum  
318 is 6,835 thousand metric tons, which is 54.20% of the total N use in the U.S. The  
319 corresponding N delivered to the Gulf of Mexico from fertilizer use in corn, soybean,  
320 wheat, and sorghum fields is 370,140 metric tons, accounting for 46.5% of the total N  
321 delivered to the Gulf of Mexico from the agricultural sector in the MRB (White et al.,  
322 2014). These solutions provide a firm footing and benchmark for the subsequent  
323 analysis of N runoff scenarios.

324 We use the historical and synthetic crop mix data to generate baseline model  
325 results as a reference point for comparison to the solutions from the climate change  
326 scenarios (column 3, Table 2). Synthetic crop acreages allow for greater model  
327 flexibility than the model that uses only historical crop mix. The added flexibility is  
328 advantageous for the scenarios with constraints or parameter values that fall outside of  
329 historically observed settings. We use these baseline results as benchmarks, rather  
330 than the results in column 1, for greater consistency between long-run equilibrium  
331 results of scenarios with and without added restrictions. The baseline N runoff to the  
332 Gulf of Mexico is 369,190 metric tons.

333

#### 334 **4.2 Results for future climate scenarios**

335 This section presents the results from the IHEAL model with predicted changes in  
336 crop yields within the MRB for 2050-2068. Table 3 shows aggregate MRB results for  
337 crop acreage and production, irrigated acreage, water use, N fertilizer use and  
338 corresponding runoff to the Gulf of Mexico under baseline and future climates.  
339 Results from five climate models, including ACCESS1.3, MIROC5, IPSL-CM5A-LR,  
340 MIROC-ESM-CHEM and CCSM4, are presented. Among these models, CCSM4 and  
341 IPSL-CM5A-LR scenarios produce the lowest and highest impacts on N runoff to the

---

<sup>2</sup> This value does not include other irrigation intensive crops like rice and alfalfa grown in the MRB.

342 Gulf. We focus our discussion of results on these models as these provide the upper  
343 and lower bounds for N runoff impacts. In addition, we also provide the results from  
344 the ensemble climate scenario where future crop yields are averages across five  
345 climate prediction models. We refer to this model as the “Ensemble Mean” in the  
346 following discussion.

347 Table 3 indicates that the impact of climate change on crop acreages and  
348 production within the MRB is mixed. Relative to the baseline with no climate change,  
349 corn acreage declines by 0.3% in CCSM4, and increases by 2.5% and 2.8% in the  
350 Ensemble Mean and IPSL-CM5A-LR, respectively. However, corn production  
351 decreases consistently in all models. Soybean acreage (production) decreases  
352 (increases) in future climates by 4.5% (5.8%) and 2.7% (5.0%) in the Ensemble Mean  
353 and IPSL-CM5A-LR, respectively. In the CCSM climate, soybean acreage increases  
354 by 0.3% and production decreases by 4.4%, respectively. Wheat acreage in future  
355 climates consistently declines relative to the baseline result. Changes in wheat  
356 production within the MRB are -4.6%, -0.9% and 5.0% under CCSM4,  
357 IPSL-CM5A-LR and the Ensemble Mean, respectively. Sorghum acreage and  
358 production decline in all models. Sorghum acreage (production) drops by 5.6%  
359 (8.3%), 16.7% (24.0%) and 5.6% (4.3%) in CCSM4, IPSL-CM5A-LR and the  
360 Ensemble Mean climates, respectively.

361 Changes in N use relative to the baseline are -0.8%, 2.2% and 1.9% in CCSM4,  
362 IPSL-CM5A-LR and the Ensemble Mean climate scenarios, respectively. Although  
363 changes in N use within the MRB are mixed across models, N delivered to the Gulf of  
364 Mexico consistently increases across all models (Table 3). Annual N runoff to the  
365 Gulf of Mexico increases compared to the baseline by 0.4% (CCSM4), 2.2%  
366 (IPSL-CM5A-LR) and 0.9% (Ensemble Mean). Although aggregate N use decreases  
367 in some models, N-intensive crop production shifts spatially to areas with high  
368 edge-of-field N leakage and Gulf runoff potential. As a result, cumulative N runoff to  
369 the Gulf increases in all models.

370 We also examine the implications of reducing N runoff to the Gulf by 45%

371 following EPA Hypoxia task force goal (Robertson and Saad, 2013) for consumer and  
372 producer surplus in each of the considered climate scenarios. We estimate the  
373 opportunity cost of reducing N runoff in terms of foregone consumer and producer  
374 surplus in the four considered commodity markets as N runoff externality is restricted.  
375 Last two rows of Table 3 show consumer and producer surplus values with and  
376 without the constraint limiting N runoff to the Gulf by 45%. The change in consumer  
377 and producer surplus estimates due to the N runoff constraint represents the  
378 opportunity cost of internalizing the N runoff externality (Xu et al., 2022). In the  
379 baseline scenario without climate change, consumer and producer surplus in the four  
380 commodity markets declines by \$7.8 billion. This estimate varies between \$6.3 and  
381 \$8.1 billion depending on climate scenario. Hence, the opportunity cost of reducing  
382 the externality by 45% can increase by 3% ( $8.1/7.8$ ) or decrease by 20% ( $6.3/7.8$ )  
383 depending on climate prediction models.

384

### 385 **4.3 N runoff with altered precipitation in the MRB and crop yields outside the** 386 **MRB**

387 Next, we extend the preceding analysis by accounting for the effects of likely  
388 changes in precipitation within the MRB and changes in crop yields outside the MRB.  
389 We use predicted precipitation for future climate scenarios as a proxy for water  
390 availability in counties with irrigated agriculture within the MRB. We obtain  
391 2050-2068 annual precipitation projections from GFDL-ESM2M-RegCM4,  
392 HadGEM2-ES-RegCM4 and MPI-ESM-LR-RegCM4 models provided by the  
393 National Center for Atmospheric Research (NCAR) (NCAR, 2022b).<sup>3</sup> We use these  
394 data to obtain mean annual precipitation across three models. Predicted changes in  
395 precipitation are combined with the baseline IHEAL water use solutions to generate

---

<sup>3</sup> RegCM4 (the Regional Climate Model version 4) is widely used to downscale global climate models for regional climate projections in the U.S. (Mei et al., 2013; Ashfaq et al., 2016). Our selection of global climate models for precipitation projection data is based on the availability of downscaled data in the NCAR database.

396 the county-scale water availability constraints for future climate change scenarios<sup>4</sup>.

397 In this analysis, we also make an effort to account for the likely change in crop  
398 yields outside the MRB. Unfortunately, we do not have data on county specific effects  
399 of climate change on crop yields outside the MRB. Although land use outside the  
400 MRB is not critical for the purposes of this study, it is important to account for yield  
401 changes outside the MRB because of implications for national commodity supply and  
402 price. Therefore, we use the result from previous literature to adjust crop yields  
403 outside the MRB uniformly (Basche et al., 2016; Karimi et al., 2017; Chen et al.,  
404 2019). In particular, we assume that corn, soybean, wheat and sorghum yields outside  
405 of MRB will change by -1.6%, -2.7%, 7.0%, and -6.0%, respectively. We apply these  
406 adjustments to all models in Table 4.

407 Table 4 presents the aggregate MRB results from five climate models and the  
408 Ensemble Mean, including crop acreage and production, irrigated acreage, water use,  
409 N use and N delivery to the Gulf of Mexico. Values in parentheses are percentage  
410 changes relative to the baseline scenario in Table 3 (no climate change). We mainly  
411 discuss the Ensemble Mean model in this section. Ensemble Mean changes in corn,  
412 soybean and wheat acreages and production are consistent with the corresponding  
413 results in Table 3 in terms of signs and magnitudes. Ensemble Mean sorghum acreage  
414 within the MRB is the same in Tables 3 and 4. However, unlike Table 3, production  
415 increases in Table 4.

416 Changes in irrigated acreage and water use relative to the baseline scenario are  
417 consistent across Ensemble Mean solutions in Tables 3 and 4. However, Ensemble  
418 Mean irrigated acreage increases while water use declines within the MRB in Table 4  
419 relative to Table 3. Two reasons explain this change. First, future precipitation is  
420 predicted to decline in counties located in Southern Kansas, Eastern New Mexico,

---

<sup>4</sup> Ensemble precipitation change is used for all climate model scenarios. A preferred approach would be to use precipitation change corresponding to each climate model used in IHEAL. Unfortunately, the precipitation prediction data for ACCESS1.3, MIROC5, IPSL-CM5A-LR, MIROC-ESM-CHEM and CCSM4 models are not available from the NCAR database.

421 Northern Texas, and Oklahoma, where agricultural production heavily relies on  
422 irrigation and precipitation. Water availability in these MRB counties decreases in  
423 Table 4 relative to Table 3, which leads to a reduction in total water use. Second,  
424 decrease in crop yields outside the MRB in Table 4 relative to Table 3 results in  
425 reallocation of some of the acreage from outside to inside the MRB. Hence, after  
426 adjusting water availability within the MRB and yields outside the MRB, acreage  
427 with irrigation increases, but total water use within the MRB declines in Table 4  
428 relative to Table 3.

429 The Ensemble Mean N fertilizer use within the MRB is 30,000 metric tons lower  
430 in Table 4 than in Table 3. However, N runoff to the Gulf of Mexico is 490 metric tons  
431 greater in Table 4 than in Table 3. Two factors contribute to this divergence between N  
432 use and runoff in the Gulf of Mexico. First, within the MRB, corn, soybean and  
433 sorghum acreages increase by 0.05, 0.11 and 0.04 million ha, respectively, while  
434 wheat acreage decreases by 0.22 million ha. Cumulatively, the acreage of these crops  
435 decreases in Table 4 relative to Table 3, which leads to the modest decline in N use.  
436 Second, the increased corn, soybean and sorghum acreages occur in regions with both  
437 higher productivity and higher N runoff potential. As a result, N runoff to the Gulf of  
438 Mexico increases from crop production within the MRB. We explore the spatial  
439 distribution of N use and associated runoff to the Gulf in the next section.

440 Table 4 also shows estimates for consumer and producer surplus changes in the  
441 four commodity markets across climate scenarios and for the corresponding 45% N  
442 runoff reduction scenarios. Estimates for consumer and producer surplus do not  
443 change significantly relative to the corresponding estimates in table 3. All estimates of  
444 consumer and producer surplus without the N runoff reduction policy decline by less  
445 than one percent relative to table 3. Similar to the results in table 3, the opportunity  
446 cost of reducing N runoff by 45% varies between \$6.4 and \$8.3 billion.

447

#### 448 **4.4 Spatial distribution of N use and delivery to the Gulf of Mexico**

449 The aggregate results show that in future climate scenarios, N delivery to the Gulf



450 of Mexico from N fertilizer use within the MRB increases relative to the baseline.  
451 However, spatial heterogeneity is observed in terms of use and runoff contribution. In  
452 this section, the spatial distribution of N use (Figure 4) and the corresponding runoff  
453 (Figure 5) to the Gulf of Mexico is discussed, using the Ensemble Mean solutions in  
454 Table 4.

455 N use declines in Oklahoma, South Dakota and Texas, where corn yields in  
456 HAWQ-SWAT Ensemble Mean climate model decline by 10.8%, 13.3% and 3.2%,  
457 respectively. In these states, lower corn yields and greater demand for irrigation  
458 increase production costs, which leads to corn production shifting to other regions.  
459 Hence, N use in these regions declines (Figure 4). However, N use increases in some  
460 areas of Colorado, Western Kansas, Iowa, Illinois, Indiana, Minnesota, North Dakota,  
461 and Wisconsin. Although corn yields in these states also decrease, the higher marginal  
462 productivity of N fertilizer in these regions leads to more corn acreage and greater N  
463 use.

464 The largest increase in N use, from 11,903 to 17,000 metric tons per year, is  
465 observed in Tazewell County, IL. This growth in N use is due to the increase in corn  
466 and wheat acreages by 13,973 and 1,430 ha, respectively. Although corn yield in this  
467 county is predicted to decline by 8.5%, acreage increases as other counties suffer even  
468 greater yield losses and reduce corn production. The largest annual N use decrease  
469 from 10,087 to 1,700 metric tons is in Reno County, KS. This decrease is due to lower  
470 corn and wheat production as yields of these crops decline by 12.9% and 5.3%,  
471 respectively. In addition, precipitation in this county also declines by 0.1%.

472 Figure 5 presents county-specific changes in N delivery to the Gulf for the  
473 Ensemble Mean analysis relative to the baseline results. Agricultural production in the  
474 UMRB and OTRB delivers most of the N runoff to the Gulf of Mexico that originates  
475 in the MRB (Kling et al., 2014). These regions are currently targeted by the EPA's  
476 Hypoxia Task Force goals to reduce N runoff. The figure shows that N runoff from  
477 the UMRB may increase with climate change, while runoff from the OTRB may  
478 decrease relative to the baseline. States located in the UMRB, including Iowa, Illinois

479 and Indiana, increase N delivery to the Gulf of Mexico relative to the baseline by  
480 3,733 metric tons, a 1.4% increase. Increased N runoff from these states accounts for  
481 99.3% of the predicted growth in N runoff to the Gulf. On the other hand, N runoff  
482 from Ohio, Tennessee and Kentucky (States located in OTRB) declines by 629 metric  
483 tons, a 2% reduction relative to the baseline runoff from these states.

484

## 485 **5. Conclusion**

486 This paper examines some of the effects of climate change on downstream water  
487 quality externality from agricultural production. Specifically, we investigate how  
488 climate-driven changes in crop yields affect agricultural production in the MRB and  
489 the corresponding water quality outcomes in the Gulf of Mexico. Our purpose is to  
490 illustrate, rather than predict, the potential impact of climate change on agricultural  
491 production externality in the form of N runoff to the Gulf. This dimension of the  
492 nexus between climate change and water resource sustainability has not received  
493 much attention in scientific literature. In this respect, our goal is to provide the first  
494 examination of its kind and spur additional research in this direction using integrated  
495 models with economic and biophysical components. The integrated approach is  
496 necessary because the behavioral response to environmental change is an important  
497 element of climate adaptation and can significantly affect downstream water quality.

498 This study differs from Metaxoglou and Smith in this volume in at least three  
499 important ways. First, we do not consider N legacy effects although it is an important  
500 part of Hypoxia in the Gulf of Mexico. Second, the IHEAL model includes N runoff  
501 from only four crops and excludes other crops and sectors including livestock and  
502 industrial production. Third, this study models N loads, while Metaxoglou and Smith  
503 investigate N concentrations. These differences imply that the results from the two  
504 studies cannot be directly compared.

505 We obtain three main findings. First, climate driven changes in crop yields affect  
506 agricultural production decisions in the MRB at intensive and extensive margins.  
507 Crop acreage and per acre N use are affected by changes in production conditions.

508 These changes increase the overall N delivery to the Gulf of Mexico from agricultural  
509 production, *ceteris paribus*. The estimated increase in N runoff to the Gulf is in the  
510 range of 0.5%-1.6% (1,690 -5,980 metric tons) relative to the baseline. These impacts  
511 are not substantial in terms of magnitude relative to current runoff. However, the  
512 corresponding marginal damages to aquatic ecosystems can be significant. Future  
513 studies should examine and evaluate the impacts of incremental increases in N runoff  
514 on Gulf aquatic ecosystems under climate change. Second, the changes in production,  
515 including N use, are spatially heterogeneous. In some counties, N use will intensify,  
516 while in others, N use will decrease. Third, spatial heterogeneity also applies at a  
517 larger spatial scale. As major contributors to the N runoff from agricultural production  
518 to the Gulf, the UMRB and OTRB are prioritized by the EPA's Hypoxia Task Force  
519 for reducing N runoff. In climate scenarios examined in this study, N runoff is  
520 expected to increase from the UMRB and decrease from the OTRB.

521 We also examine the sensitivity of the opportunity costs to reduce N runoff to the  
522 Gulf by 45% across climate scenarios. The results show that without climate change,  
523 the opportunity cost is \$7.8 billion while with climate change this estimate varies  
524 between \$6.4 and \$8.1 billion. Our N runoff reduction scenario is akin to a  
525 performance-based policy where internalizing the N runoff externality reduces N  
526 runoff by 45%. Although not directly addressed in this study, an example of a  
527 performance-based policy is tradeable pollution permit system that imposes an  
528 exogenous upper bound on environmental impact. With frictionless trade in the  
529 permits market, cost-effective distribution of production and mitigation efforts can be  
530 achieved under various emissions caps (Montgomery, 1972; Cropper and Oates, 1992).  
531 Cap and trade policies are operationally and politically challenging to implement even  
532 if technologically feasible. Nevertheless, while a detailed examination of tradable  
533 permit-based runoff mitigation is beyond the scope of this study, our results are  
534 informative in terms providing an estimate for the opportunity cost of such a policy in  
535 the four commodity markets and in terms of examining the sensitivity of the estimated  
536 costs across several climate models.

537 Several limitations of this study should be mentioned for future research. First,  
538 climate change can affect not only crop yields but also water balance. In some regions,  
539 changes in climate can influence soil water properties and surface and groundwater  
540 interactions (Scibek et al., 2007; Saha et al., 2017; Guevara-Ochoa et al., 2020). In  
541 this study, we do not account for ground versus surface water availability explicitly.  
542 Instead, precipitation changes, as predicted by the climate models included in this  
543 study and reported in the NCAR database, are used to examine the impact of changes  
544 in water availability. The explicit delineation between ground and surface water  
545 irrigation, and the associated impacts of climate change, will improve the accuracy of  
546 our estimates.

547 Second, the modeling exercise does not account for potential changes in the  
548 edge-of-field N runoff and N delivery ratios from cropland to the Gulf in future  
549 climate scenarios. This may over or underestimate N loading in the Gulf of Mexico.  
550 Unfortunately, estimates of climate impact on spatial and temporal attributes of N  
551 delivery ratios to the Gulf have not been produced yet.

552 Third, crop yield changes under future climates outside the MRB are assumed to  
553 be uniform across all counties. The assumed uniformity in yield change outside the  
554 MRB precludes the analysis of impacts on N runoff outside the MRB but is less  
555 critical for the purpose of this paper. We use these uniform yield changes outside the  
556 MRB to account for the potential effect on national commodity supply and prices  
557 which can influence production decisions within the MRB and associated N runoff.  
558 More detailed modeling of yield changes in areas outside the MRB may improve the  
559 accuracy of our estimates and enable analysis of N impacts outside of the MRB.

560 Fourth, we do not explicitly account for the effect of precipitation change in  
561 non-irrigated regions. Instead, we assume that precipitation affects water availability  
562 only in the areas with non-zero irrigation, as observed in the past data because  
563 irrigation water availability depends at least in part on precipitation. In addition, we  
564 do not explicitly account for irrigation infrastructure that links precipitation and  
565 irrigation water supply. For non-irrigated regions, we do not have estimates for the

566 effect of precipitation or irrigation on crop yields. This is an important caveat that  
567 should be addressed in future studies. A decline in precipitation in rainfed crop  
568 production regions may prompt investment in irrigation infrastructure, which we do  
569 not include in the current study. Conversely, we also do not account for potential  
570 increase in precipitation or flooding effects in non-irrigated regions that can influence  
571 production decisions and N delivery ratios.

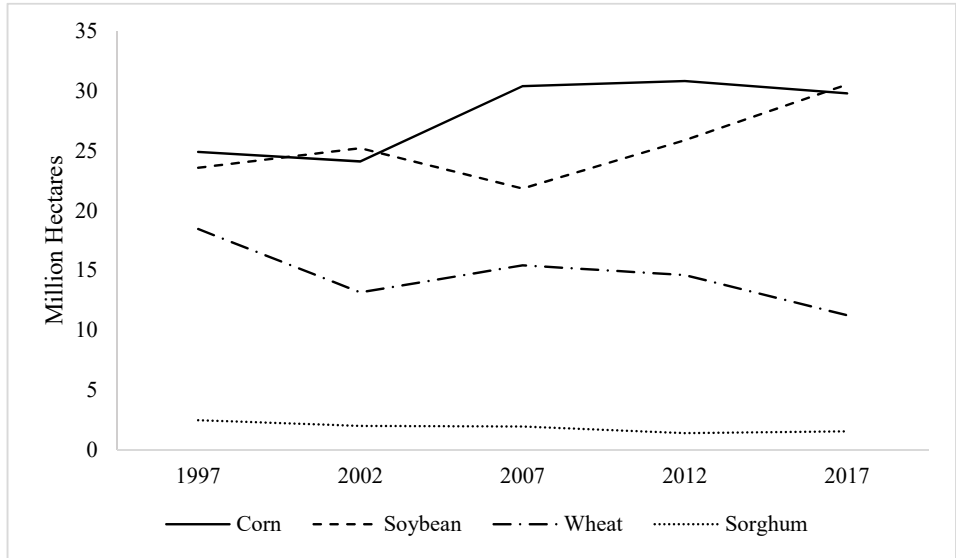
572 Fifth, the IHEAL model corresponds to the social planner's problem with perfect  
573 information. Crop production, land and input use (N and water) are obtained based on  
574 social welfare maximization. This framework is consistent with Potential Pareto  
575 Optimality criteria but does not explicitly consider implications for strict Pareto  
576 Optimality (Griffin, 1995). Nevertheless, in terms of long run equilibrium outcomes,  
577 the model provides useful insights for illustrating the potential impacts of agricultural  
578 production on downstream water quality. Such models have been extensively used for  
579 various policy-relevant analyses (Havlik et al., 2011; Chen et al., 2014; Xu et al.,  
580 2022).

581 Despite the limitations, the study provides a useful initial evaluation of the  
582 impacts of agricultural production adaptation to climate change on downstream water  
583 quality. Our purpose in this study is not to predict the water quality outcomes.  
584 Instead, our purpose is to draw attention to a previously unaddressed climate related  
585 issue, which is the externality of agricultural production adaptation to climate change  
586 in terms of nutrient runoff and downstream water quality. The initial estimates in this  
587 study show that N runoff can increase by 0.5%-1.6% (1,690 -5,980 metric tons), and  
588 reducing N runoff by 45% will be from 18.0% less to 6.4% more costly depending on  
589 climate change scenario relative to the baseline. We do not claim to have addressed  
590 this issue comprehensively, but the results suggest that future studies should examine  
591 the nutrient runoff externalities from agricultural production adaptation to climate  
592 change in greater detail.

593

594

595  
596  
597  
598  
599  
600  
601  
602  
603  
604  
605  
606  
607  
608  
609  
610  
611  
612  
613  
614  
615  
616  
617  
618



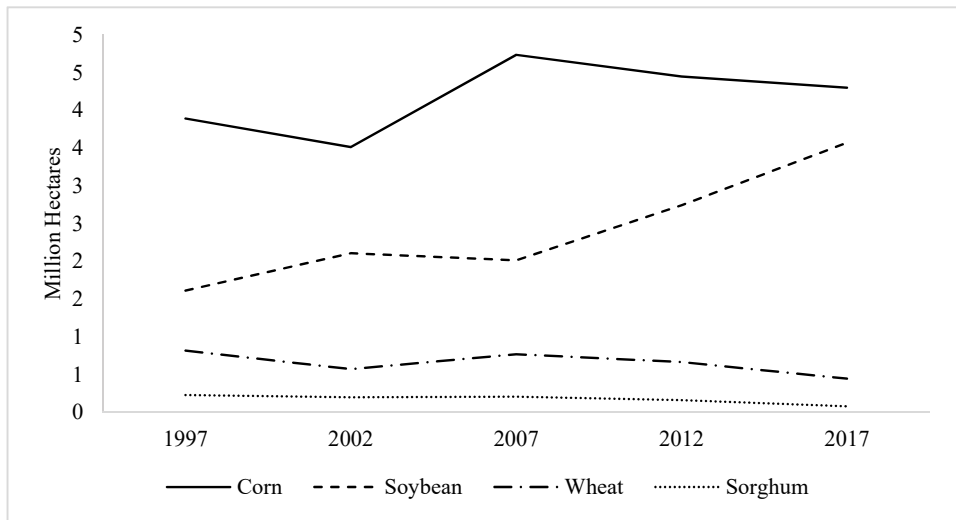
619

**Figure 1. Harvested acreage within the MRB over time (ha)**

620

621

622



623

**Figure 2. Harvested irrigated acreage within the MRB over time (ha)**

624

625

626

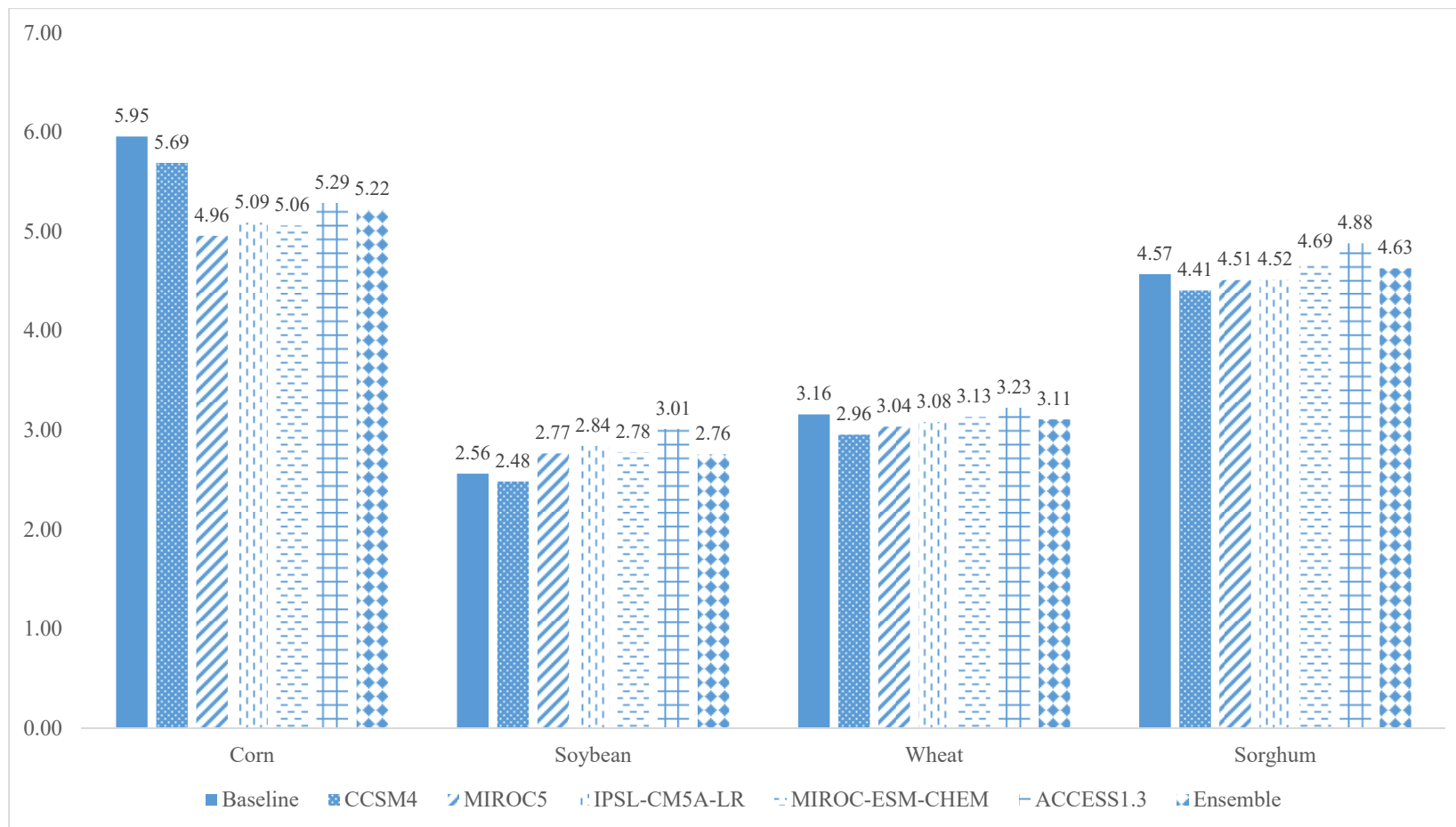


**Figure 3. The mean of crop yields under historical and future climates over all counties within the MRB (t/ha)**



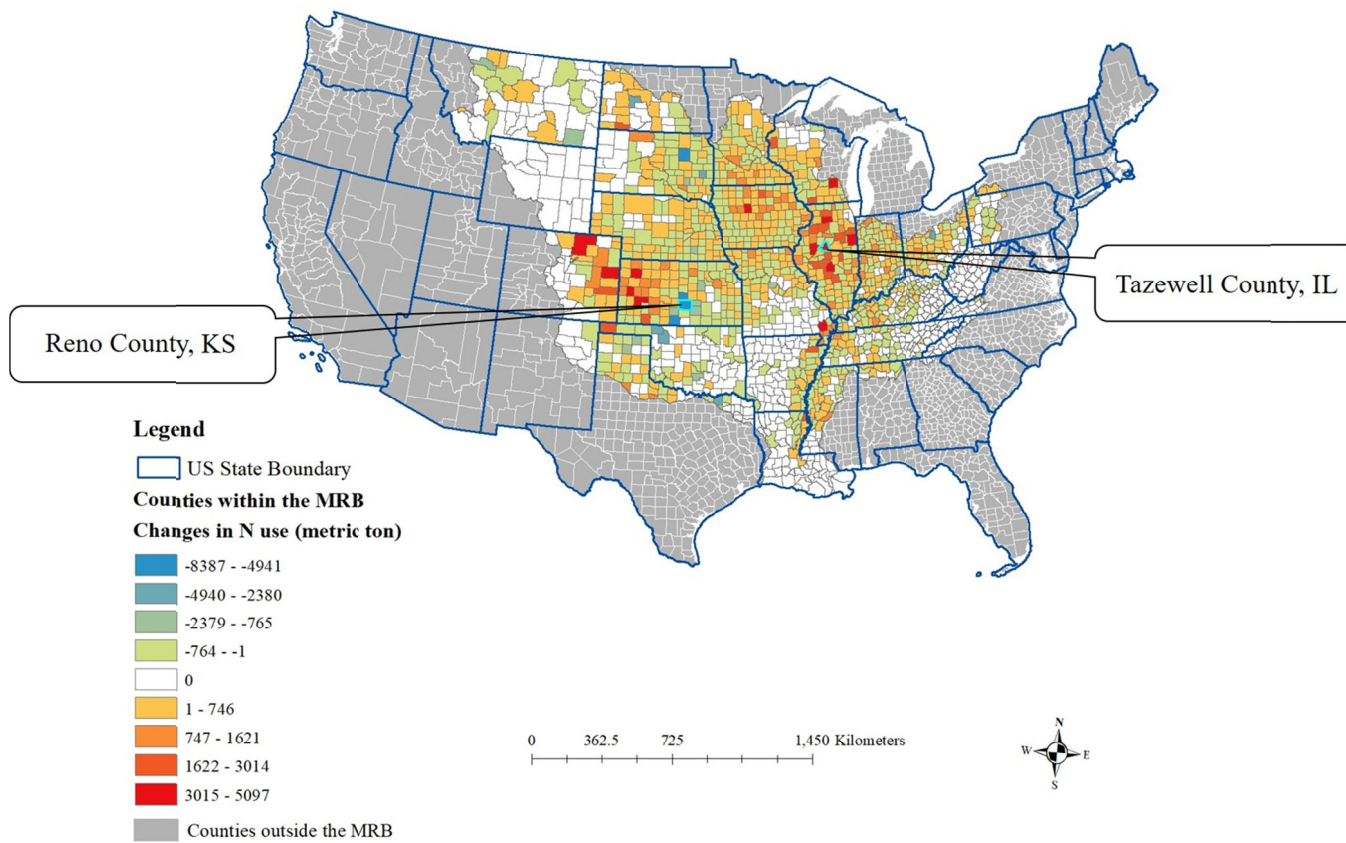


**Figure 4. Spatial distribution of N use in the Ensemble Mean of Table 4**

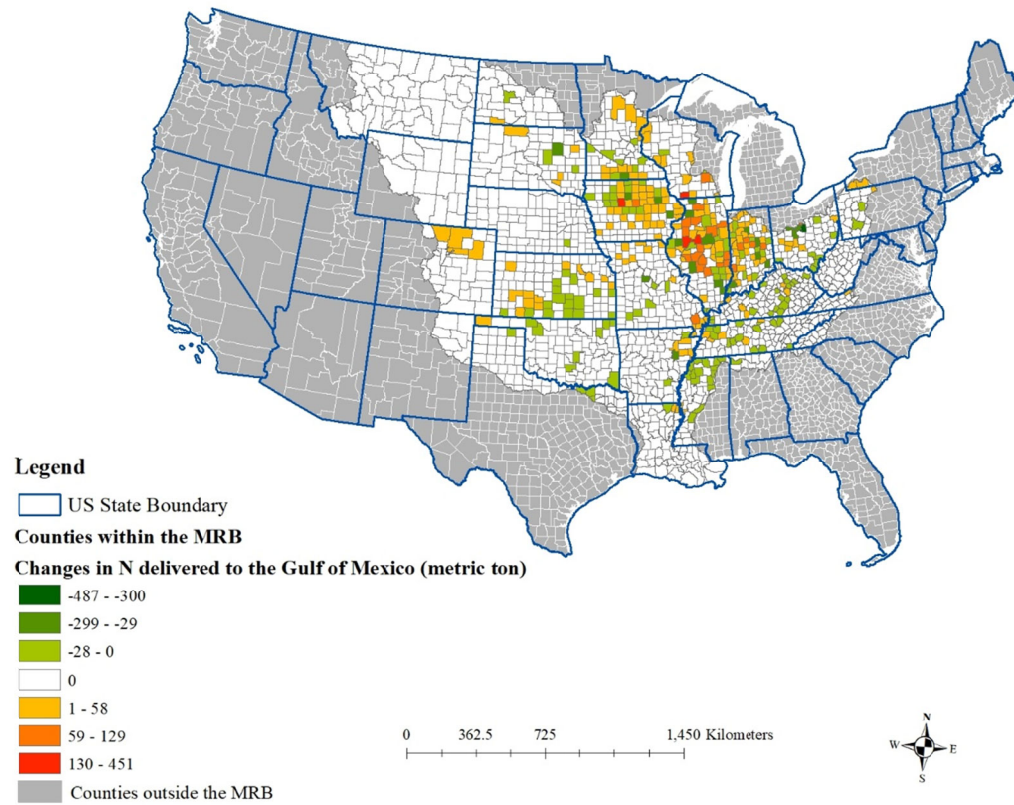


**Figure 5. Spatial distribution of N delivered to the Gulf of Mexico in the Ensemble Mean of Table 4**

**Table 1. List of climate models used in this study<sup>a</sup>**

Model	Institution	Resolution
Access1.3	CSIRO-BOM (Australia)	1.875*1.25
CCSM	NCAR (USA)	0.9*1.25
IPSL-CM5A-LR	IPSL (France)	1.875*3.75
MIROC-ESM-CHEM	MIROC (Japan)	2.8*2.8
MIROC5	MIROC (Japan)	2.8*2.8

<sup>a</sup> Source: Harding et al. (2013)

**Table 2. Validation and baseline results**

	<b>Validation results (historical crop mix)</b>	<b>Observed in 2018<sup>ab</sup></b>	<b>Baseline results (historical and synthetic crop mix)</b>
<b>LAND USE (MILLION HECTARES) FOR THE CONTIGUOUS UNITED STATES</b>			
Corn	39.6	36.0	38.2
Soybean	39.1	36.1	37.6
Winter wheat	14.5	13.2	12.4
Sorghum	2.4	2.3	2.2
<b>PRICES (\$/METRIC TON)</b>			
Corn Price	140.6	142	147.7
Soybean Price	312.6	314	335.4
Wheat Price	182.3	190	216.0
Sorghum Price	119.0	117	133.5
<b>Validation results (historical crop mix)      Values from literature      Baseline results (historical and synthetic crop mix)</b>			
Total irrigated acreage (million ha)	3.92 (MRB)	7.49 (MRB) <sup>c</sup>	3.96 (MRB)
Total water use (million acre-feet)	4.52 (MRB)	83.40 (U.S.) <sup>a</sup>	4.57 (MRB)
N applied within the MRB (1000 metric ton)	6,835 (MRB)	12,610 (U.S.) <sup>d</sup>	6,798 (MRB)
N delivered to the Gulf of Mexico from fertilizer application (metric ton)	370,140 (MRB)	796,000 (MRB) <sup>ef</sup>	369,190 (MRB)

<sup>a</sup> Source: USDA NASS, 2019

<sup>b</sup> Baseline model data, including prices and quantities for commodity demands are from 2018. Hence, we compare the baseline results with data observed in 2018.

<sup>c</sup> Total irrigated acreage of corn, soybean wheat and sorghum in the MRB in 2018 were 7,489,765 ha (USDA NASS, 2019).

<sup>d</sup> The sum of county-level farm N fertilizer use (Falcone, 2021).

<sup>e</sup> Source: White et al., 2014.

<sup>f</sup> N fertilizer use in crop production accounts for 68% of N delivered to the Gulf of Mexico from agriculture. The rest of N exported to the Gulf from agriculture comes from confined animal operations and legume crops (USGS, 2017).

**Table 3. Results under future climates**

	Baseline	Ensemble Mean	CCSM4	ACCESS1.3	IPSL-CM5A-LR	MIROC-ESM-CHEM	MIROC5
Corn acreage within the MRB (million ha)	31.6	32.5	31.5	32.8	32.4	32.8	32.5
Corn production within the MRB (million metric ton)	320.3	294.4	308.4	307.6	280.4	280.1	276.8
Soybean acreage within the MRB (million ha)	29.1	28.3	29.2	27.3	27.8	28.1	28
Soybean production within the MRB (million metric ton)	98.4	103.3	94	111.9	104.1	102	101.7
Wheat acreage within the MRB (million ha)	9.4	9.1	9.2	8.8	9.2	9.4	8.8
Wheat production within the MRB (million metric ton)	21.9	23.0	20.9	25.5	21.7	24.8	22.6
Sorghum acreage within the MRB (million ha)	1.8	1.7	1.7	1.7	1.5	1.6	1.6
Sorghum production within the MRB (million metric ton)	7.6	7.3	7	8.4	5.8	6.5	6.5
Irrigated Acreage within the MRB (ha)	3,955,607	3,979,146	3,934,678	3,953,137	3,919,521	3,922,389	3,916,433
Total water use within the MRB (million acre-feet)	4.57	4.11	4.5	4.16	4.62	4.69	4.07
N applied within the MRB (1000 metric ton)	6,798	6,930	6,747	6,931	6,948	7,006	6,874
N delivered to the Gulf of Mexico from fertilizer application (metric ton)	369,190	372,410	370,650	370,990	375,010	373,310	372,940
Consumer and producer surplus for four commodities (billion \$)	204.8	202.1	201.3	207.7	199.8	199.2	198.6
Consumer and producer surplus with a 45% N runoff reduction from MRB relative to the baseline (billion \$)	197.0	194.9	193.2	201.4	192.1	192.3	191.1

**Table 4. Results with changes in water availability and crop yields adjusted outside the MRB under future climates**

	Ensemble Mean	CCSM4	ACCESS1.3	IPSL-CM5A-LR	MIROC-ESM-CHEM	MIROC5
Corn acreage within the MRB (million ha)	32.6 (3.2%)	31.5 (-0.3%)	32.8 (3.8%)	32.5 (2.8%)	32.9 (4.1%)	32.6 (3.2%)
Corn production within the MRB (million metric ton)	294.4 (-8.1%)	308.6 (-3.7%)	307.6 (-4.0%)	280.8 (-12.3%)	280.2 (-12.5%)	277.1 (-13.5%)
Soybean acreage within the MRB (million ha)	28.4 (-2.4%)	29.2 (0.3%)	27.4 (-5.8%)	27.8 (-4.5%)	28.1 (-3.4%)	28.1 (-3.4%)
Soybean production within the MRB (million metric ton)	103.6 (5.3%)	94.1 (-4.4%)	112.2 (14.0%)	104.2 (5.9%)	102.2 (3.9%)	101.9 (3.6%)
Wheat acreage within the MRB (million ha)	8.9 (-5.3%)	8.8 (-6.4%)	8.6 (-8.5%)	8.8 (-6.4%)	8.9 (-5.3%)	8.6 (-8.5%)
Wheat production within the MRB (million metric ton)	22.4 (2.3%)	20.0 (-8.7%)	24.8 (13.2%)	20.9 (-4.6%)	23.6 (7.8%)	22.1 (0.9%)
Sorghum acreage within the MRB (million ha)	1.7 (-5.6%)	1.7 (-5.6%)	1.7 (-5.6%)	1.6 (-11.1%)	1.6 (-11.1%)	1.6 (-11.1%)
Sorghum production within the MRB (million metric ton)	7.7 (0.9%)	7.4 (-3.0%)	8.4 (10.1%)	6.5 (-14.8%)	6.7 (-12.2%)	6.8 (-10.9%)
Irrigated Acreage within the MRB (ha)	3,990,864 (0.9%)	3,949,977 (-0.1%)	3,933,342 (-0.6%)	3,937,504 (-0.5%)	3,927,531 (-0.7%)	3,922,191 (-0.8%)
Total water use within the MRB (million acre-feet)	3.91 (-14.4%)	4.45 (-2.6%)	3.90 (14.7%)	4.41 (-3.5%)	4.37 (-4.4%)	3.80 (-16.8%)
N applied within the MRB (1000 metric ton)	6,915 (1.7%)	6,720 (-1.1%)	6,912 (1.7%)	6,927 (1.9%)	6,971 (2.5%)	6,871 (1.1%)
N delivered to the Gulf of Mexico from fertilizer application (metric ton)	372,900 (1.0%)	370,880 (0.5%)	371,420 (0.6%)	375,170 (1.6%)	373,480 (1.2%)	373,050 (1.0%)
Consumer and producer surplus for four commodities (billion \$)	201.9	201.1	207.5	199.6	199.0	198.4
Consumer and producer surplus with a 45% N runoff reduction from MRB relative to the baseline (billion \$)	194.5	192.8	201.1	191.7	191.9	190.7

## Reference

- Ashfaq, M., Rastogi, D., Mei, R., Kao, S.C., Gangrade, S., Naz, B.S. and Touma, D., 2016. High-resolution ensemble projections of near-term regional climate over the continental United States. *Journal of Geophysical Research: Atmospheres*, 121(17), pp.9943-9963.
- Basche, A.D., Archontoulis, S.V., Kaspar, T.C., Jaynes, D.B., Parkin, T.B. and Miguez, F.E., 2016. Simulating long-term impacts of cover crops and climate change on crop production and environmental outcomes in the Midwestern United States. *Agriculture, Ecosystems & Environment*, 218, pp.95-106.
- Bosch, D.J., Wagena, M.B., Ross, A.C., Collick, A.S. and Easton, Z.M., 2018. Meeting water quality goals under climate change in Chesapeake Bay watershed, USA. *JAWRA Journal of the American Water Resources Association*, 54(6), pp.1239-1257.
- Chen, X. and Önal, H., 2012. Modeling agricultural supply response using mathematical programming and crop mixes. *American Journal of Agricultural Economics*, 94(3), pp.674-686.
- Chen, X., Huang, H., Khanna, M. and Önal, H., 2014. Alternative transportation fuel standards: Welfare effects and climate benefits. *Journal of Environmental Economics and Management*, 67(3), pp.241-257.
- Chen, Y., Marek, G.W., Marek, T.H., Moorhead, J.E., Heflin, K.R., Brauer, D.K., Gowda, P.H. and Srinivasan, R., 2019. Simulating the impacts of climate change on hydrology and crop production in the Northern High Plains of Texas using an improved SWAT model. *Agricultural Water Management*, 221, pp.13-24.
- Cropper, M.L. and Oates, W.E., 1992. Environmental economics: a survey. *Journal of economic literature*, 30(2), pp.675-740.
- Dieter, C.A., Linsey, K.S., Caldwell, R.R., Harris, M.A., Ivahnenko, T.I., Lovelace, J.K., Maupin, M.A. and Barber, N.L., 2018. Estimated use of water in the United States county-level data for 2015 (ver. 2.0, June 2018). US Geological Survey data release, 10, p.F7TB15V5.
- Griffin, R.C., 1995. On the meaning of economic efficiency in policy analysis. *Land Economics*, pp.1-15.
- Guevara-Ochoa, C., Medina-Sierra, A. and Vives, L., 2020. Spatio-temporal effect of climate change on water balance and interactions between groundwater and surface water in plains. *Science of the Total Environment*, 722, p.137886.
- Harding, K.J., Snyder, P.K. and Liess, S., 2013. Use of dynamical downscaling to improve the simulation of Central US warm season precipitation in CMIP5 models. *Journal of Geophysical Research: Atmospheres*, 118(22), pp.12-522.
- HAWQS, 2020, "HAWQS System and Data to model the lower 48 conterminous U.S using the SWAT model", <https://doi.org/10.18738/T8/XN3TE0>, Texas Data Repository Dataverse, V1
- Havlík, P., Schneider, U.A., Schmid, E., Böttcher, H., Fritz, S., Skalský, R., Aoki, K., De Cara, S., Kindermann, G., Kraxner, F. and Leduc, S., 2011. Global land-use implications of first and second generation biofuel targets. *Energy policy*, 39(10), pp.5690-5702.
- Ishida, K. and Jaime, M., 2015. A Partial Equilibrium of the Sorghum Markets in US, Mexico, and Japan (No. 330-2016-13894, pp. 1-1).
- Karimi, T., Stöckle, C.O., Higgins, S.S., Nelson, R.L. and Huggins, D., 2017. Projected dryland cropping system shifts in the Pacific Northwest in response to climate change. *Frontiers in Ecology and Evolution*, 5, p.20.

- Kling, C.L., Panagopoulos, Y., Rabotyagov, S.S., Valcu, A.M., Gassman, P.W., Campbell, T., White, M.J., Arnold, J.G., Srinivasan, R., Jha, M.K. and Richardson, J.J., 2014. LUMINATE: linking agricultural land use, local water quality and Gulf of Mexico hypoxia. *European Review of Agricultural Economics*, 41(3), pp.431-459.
- Kumar, S. and Merwade, V., 2011. Evaluation of NARR and CLM3. 5 outputs for surface water and energy budgets in the Mississippi River Basin. *Journal of Geophysical Research: Atmospheres*, 116(D8).
- Marshall, K. K., Riche, S. M., Seeley, R. M., Westcott, P. C. 2015. Effects of recent energy price reductions on US agriculture. United States Department of Agriculture, Economic Research Service.
- Marshall, E., Aillery, M., Ribaud, M., Key, N., Sneeringer, S., Hansen, L., Malcolm, S. and Riddle, A., 2018. Reducing nutrient losses from cropland in the Mississippi/Atchafalaya River Basin: Cost efficiency and regional distribution (No. 1477-2018-5724).
- Montgomery, W.D., 1972. Markets in licenses and efficient pollution control programs. *Journal of economic theory*, 5(3), pp.395-418.
- Mei, R., Wang, G. and Gu, H., 2013. Summer land-atmosphere coupling strength over the United States: Results from the regional climate model RegCM4-CLM3. 5. *Journal of Hydrometeorology*, 14(3), pp.946-962.
- National Center for Atmospheric Research (NCAR). 2022a. North American Regional Climate Change Assessment Program. Available at: <https://www.narccap.ucar.edu/results/index.html#climate-change>. (Accessed on March 10, 2022)
- NCAR. 2022b. Climate Data Gateway at NCAR. Available at: <https://www.earthsystemgrid.org/>. (Accessed on March 10, 2022)
- Panagopoulos, Y., Gassman, P.W., Arritt, R.W., Herzmann, D.E., Campbell, T.D., Jha, M.K., Kling, C.L., Srinivasan, R., White, M. and Arnold, J.G., 2014. Surface water quality and cropping systems sustainability under a changing climate in the Upper Mississippi River Basin. *Journal of Soil and Water Conservation*, 69(6), pp.483-494.
- Panagopoulos, Y., Gassman, P.W., Arritt, R.W., Herzmann, D.E., Campbell, T.D., Valcu, A., Jha, M.K., Kling, C.L., Srinivasan, R., White, M. and Arnold, J.G., 2015. Impacts of climate change on hydrology, water quality and crop productivity in the Ohio-Tennessee River Basin. *International Journal of Agricultural and Biological Engineering*, 8(3), pp.36-53.
- Piggott, N.E. and Wohlgenant, M.K., 2002. Price elasticities, joint products, and international trade. *Australian Journal of Agricultural and Resource Economics*, 46(4), pp.487-500.
- Robertson, D.M. and Saad, D.A., 2013. SPARROW models used to understand nutrient sources in the Mississippi/Atchafalaya River Basin. *Journal of Environmental Quality*, 42(5), pp.1422-1440.
- Saha, G.C., Li, J., Thring, R.W., Hirshfield, F. and Paul, S.S., 2017. Temporal dynamics of groundwater-surface water interaction under the effects of climate change: a case study in the Kiskatinaw River Watershed, Canada. *Journal of Hydrology*, 551, pp.440-452.
- Scibek, J., Allen, D.M., Cannon, A.J. and Whitfield, P.H., 2007. Groundwater-surface water interaction under scenarios of climate change using a high-resolution transient groundwater model. *Journal of Hydrology*, 333(2-4), pp.165-181.



- Smit, B. and Skinner, M.W., 2002. Adaptation options in agriculture to climate change: a typology. *Mitigation and adaptation strategies for global change*, 7(1), pp.85-114.
- Steiner, J.L., Devlin, D.L., Perkins, S., Aguilar, J.P., Golden, B., Santos, E.A. and Unruh, M., 2021. Policy, Technology, and Management Options for Water Conservation in the Ogallala Aquifer in Kansas, USA. *Water*, 13(23), p.3406.
- U.S. Environmental Protection Agency (US EPA). 2014. Mississippi River Gulf of Mexico Watershed Nutrient Task Force New Goal Framework. <https://www.epa.gov/sites/production/files/2015-07/documents/htf-goals-framework-2015.pdf>. (Accessed on Dec 2021)
- US EPA. 2019. Hypoxia 101. <https://www.epa.gov/ms-htf/hypoxia-101>. (Accessed on Dec 2021)
- US EPA. 2021a. Northern Gulf of Mexico Hypoxic Zone. Available at: <https://www.epa.gov/ms-htf/northern-gulf-mexico-hypoxic-zone>. (Accessed on Dec 2021)
- US EPA. 2021b. Hypoxia Task Force Nutrient Reduction Strategies. Available at: <https://www.epa.gov/ms-htf/hypoxia-task-force-nutrient-reduction-strategies>. (Accessed on Dec 2021)
- USDA ERS (United States Department of Agriculture Economic Research Service). 2019. Fertilizer Use and Price. <https://www.ers.usda.gov/data-products/fertilizer-use-and-price>. (accessed 30 Oct 2019).
- USDA ERS. 2021. Irrigation & Water Use. Available at: <https://www.ers.usda.gov/topics/farm-practices-management/irrigation-water-use/>. (Accessed on Dec 2021)
- USDA ERS. 2022. Irrigated cropping patterns in the United States have evolved significantly since 1964. Available at: <https://www.ers.usda.gov/data-products/chart-gallery/gallery/chart-detail/?chartId=103568>. (Accessed on July 2022)
- U.S. Department of Agriculture National Agricultural Statistics Service (USDA NASS). 2019. 2017 Census of Agriculture. Available at: [www.nass.usda.gov/AgCensus](http://www.nass.usda.gov/AgCensus). (Accessed on Dec 2021)
- USDA NASS. 2020. U.S. & All States County Data – Crops. Washington, DC. <http://www.nass.usda.gov/>. (accessed 13 May 2021).
- U.S. Geological Survey (USGS). 2018. Water-use data available from USGS. <https://water.usgs.gov/watuse/data/index.html>. (accessed 1 Jan 2022).
- Westcott, P.C. and Hoffman, L.A., 1999. Price determination for corn and wheat: the role of market factors and government programs (No. 1488-2016-123383).
- White, M.J., Santhi, C., Kannan, N., Arnold, J.G., Harmel, D., Norfleet, L., Allen, P., DiLuzio, M., Wang, X., Atwood, J. and Haney, E., 2014. Nutrient delivery from the Mississippi River to the Gulf of Mexico and effects of cropland conservation. *Journal of Soil and Water Conservation*, 69(1), pp.26-40.
- Wu, D., Qu, J.J. and Hao, X., 2015. Agricultural drought monitoring using MODIS-based drought indices over the USA Corn Belt. *International Journal of Remote Sensing*, 36(21), pp.5403-5425.
- Xu, Y., Bosch, D.J., Wagena, M.B., Collick, A.S. and Easton, Z.M., 2019. Meeting water quality goals by spatial targeting of best management practices under climate change. *Environmental management*, 63(2), pp.173-184.
- Xu, Y., Elbakidze, L., Yen, H., Arnold, J.G., Gassman, P.W., Hubbard, J. and Strager,

M.P., 2022. Integrated assessment of nitrogen runoff to the Gulf of Mexico. Resource and Energy Economics, 67, p.101279.

### Appendix

$$\max_{x, n_1, n_2, w_1} \pi = \int_0^x p(t) dt - C_n * (n_1 + n_2) - C_w * w_1 \quad (S1)$$

subject to

$$\alpha_1 * f(n_1, w_1) + \alpha_2 * g(n_2) \geq x \quad (S2)$$

Lagrangian and corresponding first order conditions are as follows:

$$L = \int_0^x p(t) dt - C_n * (n_1 + n_2) - C_w * w_1 + \lambda(\alpha_1 * f(n_1, w_1) + \alpha_2 * g(n_2) - x) \quad (S3)$$

$$[x] \quad \frac{\partial L}{\partial x} = p(x) - \lambda = 0 \quad (S4)$$

$$[n_1] \quad \frac{\partial L}{\partial n_1} = -C_n + \lambda \alpha_1 f_{n_1} = 0$$

$$[n_2] \quad \frac{\partial L}{\partial n_2} = -C_n + \lambda \alpha_2 g_{n_2} = 0$$

$$[w_1] \quad \frac{\partial L}{\partial w_1} = -C_w + \lambda \alpha_1 f_{w_1} = 0$$

$$[\lambda] \quad \frac{\partial L}{\partial \lambda} = \alpha_1 * f(n_1, w_1) + \alpha_2 * g(n_2) - x = 0$$

Total differentiation of the first order conditions with respect to  $\alpha_1$  gives:

$$[x] \quad p_x \frac{\partial x}{\partial \alpha_1} - \frac{\partial \lambda}{\partial \alpha_1} = 0 \quad (S5)$$

$$[n_1] \quad \lambda \alpha_1 f_{n_1 n_1} \frac{\partial n_1}{\partial \alpha_1} + \lambda \alpha_1 f_{n_1 w_1} \frac{\partial w_1}{\partial \alpha_1} + \alpha_1 f_{n_1} \frac{\partial \lambda}{\partial \alpha_1} = -\lambda f_{n_1}$$

$$[n_2] \quad \lambda \alpha_2 g_{n_2 n_2} \frac{\partial n_2}{\partial \alpha_1} + \alpha_2 g_{n_2} \frac{\partial \lambda}{\partial \alpha_1} = 0$$

$$[w_1] \quad \lambda \alpha_1 f_{w_1 n_1} \frac{\partial n_1}{\partial \alpha_1} + \lambda \alpha_1 f_{w_1 w_1} \frac{\partial w_1}{\partial \alpha_1} + \alpha_1 f_{w_1} \frac{\partial \lambda}{\partial \alpha_1} = -\lambda f_{w_1}$$

$$[\lambda] \quad \alpha_1 f_{n_1} \frac{\partial n_1}{\partial \alpha_1} + \alpha_1 f_{w_1} \frac{\partial w_1}{\partial \alpha_1} + \alpha_2 g_{n_2} \frac{\partial n_2}{\partial \alpha_1} - \frac{\partial x}{\partial \alpha_1} = -f(n_1, w_1)$$

The second order conditions can be expressed in terms of the Bordered Hessian representation as  $AH = B$ , where

$A = \left[ \frac{\partial x}{\partial \alpha_1}, \frac{\partial n_1}{\partial \alpha_1}, \frac{\partial n_2}{\partial \alpha_1}, \frac{\partial w_1}{\partial \alpha_1}, \frac{\partial \lambda}{\partial \alpha_1} \right]$  is the vector of derivatives of all endogenous variables w.r.t  $\tau$ .  $H$  is the Hessian matrix shown below, and  $B = [0, -\lambda f_{n_1}, 0, -\lambda f_{w_1}, -f(n_1, w_1)]$ .

$$H = \begin{bmatrix} p_x & 0 & 0 & 0 & -1 \\ 0 & \lambda \alpha_1 f_{n_1 n_1} & 0 & \lambda \alpha_1 f_{w_1 n_1} & \alpha_1 f_{n_1} \\ 0 & 0 & \lambda \alpha_2 g_{n_2 n_2} & 0 & \alpha_2 g_{n_2} \\ 0 & \lambda \alpha_1 f_{n_1 w_1} & 0 & \lambda \alpha_1 f_{w_1 w_1} & \alpha_1 f_{w_1} \\ -1 & \alpha_1 f_{n_1} & \alpha_2 g_{n_2} & \alpha_1 f_{w_1} & 0 \end{bmatrix} \quad (S6)$$

$$|H| = \alpha_1^2 \alpha_2 \lambda^2 \left[ 2\alpha_1 f_{n_1} f_{n_1 w_1} f_{w_1} g_{n_2 n_2} p_x - \alpha_1 f_{n_1}^2 f_{w_1 w_1} g_{n_2 n_2} p_x + f_{n_1 w_1}^2 (\lambda g_{n_2 n_2} + \alpha_2 p_x g_{n_2}^2) - f_{n_1 n_1} (\lambda f_{w_1 w_1} g_{n_2 n_2} + \alpha_2 f_{w_1 w_1} p_x g_{n_2}^2 + \alpha_1 f_{w_1}^2 g_{n_2 n_2} p_x) \right] \quad (S7)$$

$$\frac{\partial n_1}{\partial \alpha_1} = \frac{|H_{n_1}|}{|H|}$$

$$\begin{aligned} & \frac{-\alpha_1 \alpha_2 \lambda^2 (f_{n_1 w_1} f_{w_1} - f_{n_1} f_{w_1 w_1}) (\alpha_2 p_x g_{n_2}^2 + g_{n_2 n_2} (\lambda + \alpha_1 p_x f(n_1, w_1)))}{\alpha_1^2 \alpha_2 \lambda^2 \left[ 2\alpha_1 f_{n_1} f_{n_1 w_1} f_{w_1} g_{n_2 n_2} p_x - \alpha_1 f_{n_1}^2 f_{w_1 w_1} g_{n_2 n_2} p_x + f_{n_1 w_1}^2 (\lambda g_{n_2 n_2} + \alpha_2 p_x g_{n_2}^2) - f_{n_1 n_1} (\lambda f_{w_1 w_1} g_{n_2 n_2} + \alpha_2 f_{w_1 w_1} p_x g_{n_2}^2 + \alpha_1 f_{w_1}^2 g_{n_2 n_2} p_x) \right]} \\ & \frac{- (f_{n_1 w_1} f_{w_1} - f_{n_1} f_{w_1 w_1}) (\alpha_2 p_x g_{n_2}^2 + g_{n_2 n_2} (\lambda + \alpha_1 p_x f(n_1, w_1)))}{\alpha_1 \left[ 2\alpha_1 f_{n_1} f_{n_1 w_1} f_{w_1} g_{n_2 n_2} p_x - \alpha_1 f_{n_1}^2 f_{w_1 w_1} g_{n_2 n_2} p_x + f_{n_1 w_1}^2 (\lambda g_{n_2 n_2} + \alpha_2 p_x g_{n_2}^2) - f_{n_1 n_1} (\lambda f_{w_1 w_1} g_{n_2 n_2} + \alpha_2 f_{w_1 w_1} p_x g_{n_2}^2 + \alpha_1 f_{w_1}^2 g_{n_2 n_2} p_x) \right]} \end{aligned} \quad (S8)$$

$$\begin{aligned}
\frac{\partial n_2}{\partial \alpha_1} &= \frac{|H_{n_2}|}{|H|} \\
&= \frac{-\alpha_1^2 \alpha_2 \lambda^2 g_{n_2} p_x \left[ -2f_{n_1} f_{n_1 w_1} f_{w_1} + f_{n_1 n_1} f_{w_1}^2 + f(n_1, w_1) (f_{n_1 w_1}^2 - f_{n_1 n_1} f_{w_1 w_1}) \right]}{\alpha_1^2 \alpha_2 \lambda^2 \left[ 2\alpha_1 f_{n_1} f_{n_1 w_1} f_{w_1} g_{n_2 n_2} p_x - \alpha_1 f_{n_1}^2 f_{w_1 w_1} g_{n_2 n_2} p_x + f_{n_1 w_1}^2 (\lambda g_{n_2 n_2} + \alpha_2 p_x g_{n_2}^2) - f_{n_1 n_1} (\lambda f_{w_1 w_1} g_{n_2 n_2} + \alpha_2 f_{w_1 w_1} p_x g_{n_2}^2 + \alpha_1 f_{w_1}^2 g_{n_2 n_2} p_x) \right]} \\
&= \frac{-g_{n_2} p_x \left[ -2f_{n_1} f_{n_1 w_1} f_{w_1} + f_{n_1 n_1} f_{w_1}^2 + f(n_1, w_1) (f_{n_1 w_1}^2 - f_{n_1 n_1} f_{w_1 w_1}) \right]}{2\alpha_1 f_{n_1} f_{n_1 w_1} f_{w_1} g_{n_2 n_2} p_x - \alpha_1 f_{n_1}^2 f_{w_1 w_1} g_{n_2 n_2} p_x + f_{n_1 w_1}^2 (\lambda g_{n_2 n_2} + \alpha_2 p_x g_{n_2}^2) - f_{n_1 n_1} (\lambda f_{w_1 w_1} g_{n_2 n_2} + \alpha_2 f_{w_1 w_1} p_x g_{n_2}^2 + \alpha_1 f_{w_1}^2 g_{n_2 n_2} p_x)} \quad (S9)
\end{aligned}$$

$$\begin{aligned}
\frac{\partial w_1}{\partial \alpha_1} &= \frac{|H_{w_1}|}{|H|} \\
&= \frac{-\lambda^2 \alpha_1 \alpha_2 (f_{n_1 w_1} f_{n_1} - f_{w_1} f_{n_1 n_1}) (\alpha_2 p_x g_{n_2}^2 + g_{n_2 n_2} (\lambda + \alpha_1 p_x f(n_1, w_1)))}{\alpha_1^2 \alpha_2 \lambda^2 \left[ 2\alpha_1 f_{n_1} f_{n_1 w_1} f_{w_1} g_{n_2 n_2} p_x - \alpha_1 f_{n_1}^2 f_{w_1 w_1} g_{n_2 n_2} p_x + f_{n_1 w_1}^2 (\lambda g_{n_2 n_2} + \alpha_2 p_x g_{n_2}^2) - f_{n_1 n_1} (\lambda f_{w_1 w_1} g_{n_2 n_2} + \alpha_2 f_{w_1 w_1} p_x g_{n_2}^2 + \alpha_1 f_{w_1}^2 g_{n_2 n_2} p_x) \right]} \\
&= \frac{-(f_{n_1 w_1} f_{n_1} - f_{w_1} f_{n_1 n_1}) (\alpha_2 p_x g_{n_2}^2 + g_{n_2 n_2} (\lambda + \alpha_1 p_x f(n_1, w_1)))}{\alpha_1 \left[ 2\alpha_1 f_{n_1} f_{n_1 w_1} f_{w_1} g_{n_2 n_2} p_x - \alpha_1 f_{n_1}^2 f_{w_1 w_1} g_{n_2 n_2} p_x + f_{n_1 w_1}^2 (\lambda g_{n_2 n_2} + \alpha_2 p_x g_{n_2}^2) - f_{n_1 n_1} (\lambda f_{w_1 w_1} g_{n_2 n_2} + \alpha_2 f_{w_1 w_1} p_x g_{n_2}^2 + \alpha_1 f_{w_1}^2 g_{n_2 n_2} p_x) \right]} \quad (S10)
\end{aligned}$$

Total differentiation of the first order conditions with respect to  $\alpha_2$  gives:

$$[x] \quad p_x \frac{\partial x}{\partial \alpha_2} - \frac{\partial \lambda}{\partial \alpha_2} = 0 \quad (S11)$$

$$[n_1] \quad \lambda \alpha_1 f_{n_1 n_1} \frac{\partial n_1}{\partial \alpha_2} + \lambda \alpha_1 f_{n_1 w_1} \frac{\partial w_1}{\partial \alpha_2} + \alpha_1 f_{n_1} \frac{\partial \lambda}{\partial \alpha_2} = 0$$

$$[n_2] \quad \lambda \alpha_2 g_{n_2 n_2} \frac{\partial n_2}{\partial \alpha_2} + \alpha_2 g_{n_2} \frac{\partial \lambda}{\partial \alpha_2} = -\lambda g_{n_2}$$

$$[w_1] \quad \lambda \alpha_1 f_{w_1 n_1} \frac{\partial n_1}{\partial \alpha_2} + \lambda \alpha_1 f_{w_1 w_1} \frac{\partial w_1}{\partial \alpha_2} + \alpha_1 f_{w_1} \frac{\partial \lambda}{\partial \alpha_2} = 0$$

$$[\lambda] \quad \alpha_1 f_{n_1} \frac{\partial n_1}{\partial \alpha_2} + \alpha_1 f_{w_1} \frac{\partial w_1}{\partial \alpha_2} + \alpha_2 g_{n_2} \frac{\partial n_2}{\partial \alpha_2} - \frac{\partial x_1}{\partial \alpha_2} = -g(n_2)$$

The second order conditions can be expressed in terms of the Bordered Hessian representation as  $AH = B$ , where  $A = \left[ \frac{\partial x}{\partial \alpha_2}, \frac{\partial n_1}{\partial \alpha_2}, \frac{\partial n_2}{\partial \alpha_2}, \frac{\partial w_1}{\partial \alpha_2}, \frac{\partial \lambda}{\partial \alpha_2} \right]$  is the vector of derivatives of all endogenous variables w.r.t  $\tau$ .  $H$  is the Hessian matrix shown below, and  $B = [0, 0, -\lambda g_{n_2}, 0, -g(n_2)]$ .

$$H = \begin{bmatrix} p_{x_1} & 0 & 0 & 0 & -1 \\ 0 & \lambda \alpha_1 f_{n_1 n_1} & 0 & \lambda \alpha_1 f_{w_1 n_1} & \alpha_1 f_{n_1} \\ 0 & 0 & \lambda \alpha_2 g_{n_2 n_2} & 0 & \alpha_2 g_{n_2} \\ 0 & \lambda \alpha_1 f_{n_1 w_1} & 0 & \lambda \alpha_1 f_{w_1 w_1} & \alpha_1 f_{w_1} \\ -1 & \alpha_1 f_{n_1} & \alpha_2 g_{n_2} & \alpha_1 f_{w_1} & 0 \end{bmatrix} \quad (S12)$$

$$|H| = \alpha_1^2 \alpha_2 \lambda^2 \left[ 2\alpha_1 f_{n_1} f_{n_1 w_1} f_{w_1} g_{n_2 n_2} p_x - \alpha_1 f_{n_1}^2 f_{w_1 w_1} g_{n_2 n_2} p_x + f_{n_1 w_1}^2 (\lambda g_{n_2 n_2} + \alpha_2 p_x g_{n_2}^2) - f_{n_1 n_1} (\lambda f_{w_1 w_1} g_{n_2 n_2} + \alpha_2 f_{w_1 w_1} p_x g_{n_2}^2 + \alpha_1 f_{w_1}^2 g_{n_2 n_2} p_x) \right] \quad (S13)$$

$$\frac{\partial n_1}{\partial \alpha_2} = \frac{|H_{n_1}|}{|H|}$$

$$= \frac{\alpha_1^2 \alpha_2 \lambda^2 p_x (f_{n_1 w_1} f_{w_1} - f_{n_1} f_{w_1 w_1})}{\alpha_1^2 \alpha_2 \lambda^2 \left[ 2\alpha_1 f_{n_1} f_{n_1 w_1} f_{w_1} g_{n_2 n_2} p_x - \alpha_1 f_{n_1}^2 f_{w_1 w_1} g_{n_2 n_2} p_x + f_{n_1 w_1}^2 (\lambda g_{n_2 n_2} + \alpha_2 p_x g_{n_2}^2) - f_{n_1 n_1} (\lambda f_{w_1 w_1} g_{n_2 n_2} + \alpha_2 f_{w_1 w_1} p_x g_{n_2}^2 + \alpha_1 f_{w_1}^2 g_{n_2 n_2} p_x) \right]}$$

$$= \frac{p_x (f_{n_1 w_1} f_{w_1} - f_{n_1} f_{w_1 w_1})}{\left[ 2\alpha_1 f_{n_1} f_{n_1 w_1} f_{w_1} g_{n_2 n_2} p_x - \alpha_1 f_{n_1}^2 f_{w_1 w_1} g_{n_2 n_2} p_x + f_{n_1 w_1}^2 (\lambda g_{n_2 n_2} + \alpha_2 p_x g_{n_2}^2) - f_{n_1 n_1} (\lambda f_{w_1 w_1} g_{n_2 n_2} + \alpha_2 f_{w_1 w_1} p_x g_{n_2}^2 + \alpha_1 f_{w_1}^2 g_{n_2 n_2} p_x) \right]} \quad (S14)$$

$$\begin{aligned} \frac{\partial n_2}{\partial \alpha_2} &= \frac{|H_{n_2}|}{|H|} \\ &= \frac{\alpha_1^2 g_{n_2} \lambda^2 \left[ -2\alpha_1 f_{n_1} f_{n_1 w_1} f_{w_1} p_x + \alpha_1 f_{n_1}^2 f_{w_1 w_1} g_{n_2 n_2} p_x - f_{n_1 w_1}^2 (\lambda + \alpha_2 p_x g(n_2)) + f_{n_1 n_1} (\lambda f_{w_1 w_1} + \alpha_1 f_{w_1}^2 p_x + \alpha_2 f_{w_1 w_1} g_{n_2} p_x) \right]}{\alpha_1^2 \alpha_2 \lambda^2 \left[ 2\alpha_1 f_{n_1} f_{n_1 w_1} f_{w_1} g_{n_2 n_2} p_x - \alpha_1 f_{n_1}^2 f_{w_1 w_1} g_{n_2 n_2} p_x + f_{n_1 w_1}^2 (\lambda g_{n_2 n_2} + \alpha_2 p_x g_{n_2}^2) - f_{n_1 n_1} (\lambda f_{w_1 w_1} g_{n_2 n_2} + \alpha_2 f_{w_1 w_1} p_x g_{n_2}^2 + \alpha_1 f_{w_1}^2 g_{n_2 n_2} p_x) \right]} \\ &= \frac{g_{n_2} \left[ -2\alpha_1 f_{n_1} f_{n_1 w_1} f_{w_1} p_x + \alpha_1 f_{n_1}^2 f_{w_1 w_1} g_{n_2 n_2} p_x - f_{n_1 w_1}^2 (\lambda + \alpha_2 p_x g(n_2)) + f_{n_1 n_1} (\lambda f_{w_1 w_1} + \alpha_1 f_{w_1}^2 p_x + \alpha_2 f_{w_1 w_1} g_{n_2} p_x) \right]}{\alpha_2 \left[ 2\alpha_1 f_{n_1} f_{n_1 w_1} f_{w_1} g_{n_2 n_2} p_x - \alpha_1 f_{n_1}^2 f_{w_1 w_1} g_{n_2 n_2} p_x + f_{n_1 w_1}^2 (\lambda g_{n_2 n_2} + \alpha_2 p_x g_{n_2}^2) - f_{n_1 n_1} (\lambda f_{w_1 w_1} g_{n_2 n_2} + \alpha_2 f_{w_1 w_1} p_x g_{n_2}^2 + \alpha_1 f_{w_1}^2 g_{n_2 n_2} p_x) \right]} \quad (S15) \end{aligned}$$

$$\begin{aligned} \frac{\partial w_1}{\partial \alpha_2} &= \frac{|H_{w_1}|}{|H|} \\ &= \frac{\alpha_1^2 \alpha_2 \lambda^2 p_x (f_{n_1 w_1} f_{n_1} - f_{w_1} f_{n_1 n_1}) (g_{n_2}^2 - g(n_2) g_{n_2 n_2})}{\alpha_1^2 \alpha_2 \lambda^2 \left[ 2\alpha_1 f_{n_1} f_{n_1 w_1} f_{w_1} g_{n_2 n_2} p_x - \alpha_1 f_{n_1}^2 f_{w_1 w_1} g_{n_2 n_2} p_x + f_{n_1 w_1}^2 (\lambda g_{n_2 n_2} + \alpha_2 p_x g_{n_2}^2) - f_{n_1 n_1} (\lambda f_{w_1 w_1} g_{n_2 n_2} + \alpha_2 f_{w_1 w_1} p_x g_{n_2}^2 + \alpha_1 f_{w_1}^2 g_{n_2 n_2} p_x) \right]} \\ &= \frac{p_x (f_{n_1 w_1} f_{n_1} - f_{w_1} f_{n_1 n_1}) (g_{n_2}^2 - g(n_2) g_{n_2 n_2})}{\left[ 2\alpha_1 f_{n_1} f_{n_1 w_1} f_{w_1} g_{n_2 n_2} p_x - \alpha_1 f_{n_1}^2 f_{w_1 w_1} g_{n_2 n_2} p_x + f_{n_1 w_1}^2 (\lambda g_{n_2 n_2} + \alpha_2 p_x g_{n_2}^2) - f_{n_1 n_1} (\lambda f_{w_1 w_1} g_{n_2 n_2} + \alpha_2 f_{w_1 w_1} p_x g_{n_2}^2 + \alpha_1 f_{w_1}^2 g_{n_2 n_2} p_x) \right]} \quad (S16) \end{aligned}$$